

Received: 15 May 2007,

Revised: 3 September 2007,

Accepted: 14 September 2007,

Published online in Wiley InterScience: 4 December 2007

(www.interscience.wiley.com) DOI 10.1002/poc.1278

Deprotonation and radicalization of glycine neutral structures

Gang Yang^{a,b}, Yuangang Zu^{a*} and Lijun Zhou^a

Ab initio calculations at MP2/6-311++G(d,p) theoretical level were performed to study the deprotonation and radicalization processes of 13 glycine neutral structures (A. G. Császár, *J. Am. Chem. Soc.* 1992; 114: 9568). The deprotonation processes to glycine neutral structures take place at the carboxylic sites instead of α -C or amido sites. Two carboxylic deprotonated structures were obtained with the deprotonation energies calculated within the range of 1413.27–1460.03 kJ · mol^{−1}, which are consistent with the experimental results. However, the radicalization processes will take place at the α -C rather than carboxylic O or amido sites, agreeing with the experimental results. Seven α -C radicals were obtained with the radical stabilization energies calculated within the range of 44.87–111.78 kJ · mol^{−1}. The population analyses revealed that the main conformations of the neutral or radical state are constituted by several stable structures, that is, the other structures can be excluded from the future considerations and thus save computational resources. Copyright © 2007 John Wiley & Sons, Ltd.

Keywords: *ab initio* calculations; deprotonation energy; conformational analysis; population; radical stabilization energy

INTRODUCTION

Protonation, deprotonation and radicalization are three elementary processes in chemistry and biology. At molecular level, they are closely related to protein function and enzyme catalysis. Amino acids are the building blocks of proteins and have long served as the models of proteins.^[1–4] Glycine, the simplest amino acids, exists in the neutral form ($\text{NH}_2\text{—CH}_2\text{—COOH}$) in gas phase.^[5] The neutral conformations of glycine have been subjected to many experimental and theoretical investigations.^[6–20] In the landmark contribution, Császár^[10] adopted MP2/6-311++G(d,p) methods to study the neutral glycine conformations and located 13 stationary points on the potential energy surface, shown in Fig. 1.

Apart from the neutral structures, the protonated conformations of glycine have also been clearly understood at molecular level.^[15–19] At HF/6-31G(d) theoretical level, nine stationary points were determined on potential energy surface for the protonated glycine, with three of amino N-protonated and six of carbonyl O-protonated structures, respectively.^[16] At higher level MP2/6-311+G(d,p) theory, Zhang *et al.*^[19] continued the protonation studies and obtained eight energy minima, concluding that the global minimum on potential energy surface should be an amino N-protonated conformer containing hydrogen bonding between $—\text{NH}_3^+$ and $\text{O}=\text{C}<$ groups. As to glycine radical structures, much fewer studies were made up to date.^[18,20,21] In the previous work of Croft *et al.*,^[20] only the α -C radical to the most stable neutral structure Neu^A was taken into calculations using B3LYP/6-31(d) methods. By means of BLYP/SVP methods, Mavrandakis *et al.*^[21] investigated the mutual interactions between carbon nanotubes and glycine α -C and amido radicals; however, the radicals they considered were also limited to the most stable neutral structure Neu^A. It is therefore of high value to perform a comprehensive research on glycine radicals, including the carboxylic O radicals ($\text{NH}_2\text{CH}_2\text{COO}^\cdot$). The motivation of studying O radicals is that they are found as widely as C radicals in chemistry and biology. In addition, the theoretical methods previously adopted are of relatively low levels, 6-31G(d)

basis set used in References^[18,20] and BLYP functional used in Reference.^[21] To the best of our knowledge, only one deprotonated structure of glycine was previously obtained at MP2/6-31G(d) theoretical level.^[18] Foremost, the geometries of anions such as glycine deprotonated structures are heavily dependent on the diffuse functions which are absent in that work.^[18] Accordingly, further studies on glycine deprotonated structures are absolutely necessary.

As aforementioned, the studies with high-level *ab initio* methods will be performed on glycine radical and deprotonated structures. On such basis, the deprotonated and radical structures were then correlated with their corresponding neutral structures through the parameters of deprotonation energies and radical stabilization energies (RSE), respectively. In the end, the populations were evaluated for glycine neutral, deprotonated and radical structures.

COMPUTATIONAL METHODS

All the theoretical calculations were performed using Gaussian 98 program.^[22] In accordance with Reference,^[10] MP2/6-311++G(d,p) theoretical methods were used for the main discussions. It was noted that 6-311++G(d,p) is a triple- ζ basis set supplemented with diffusion and polarization functions on both heavy and hydrogen atoms.

* Key Laboratory of Forest Plant Ecology, Ministry of Education, Northeast Forestry University, Harbin 150040, P. R. China.
E-mail: theobiochem@gmail.com

a G. Yang, Y. Zu, L. Zhou
Key Laboratory of Forest Plant Ecology, Ministry of Education, Northeast Forestry University, Harbin 150040, P. R. China

b G. Yang
Dalian Institute of Chemical Physics, Chinese Academy of Sciences, Dalian 116023, China

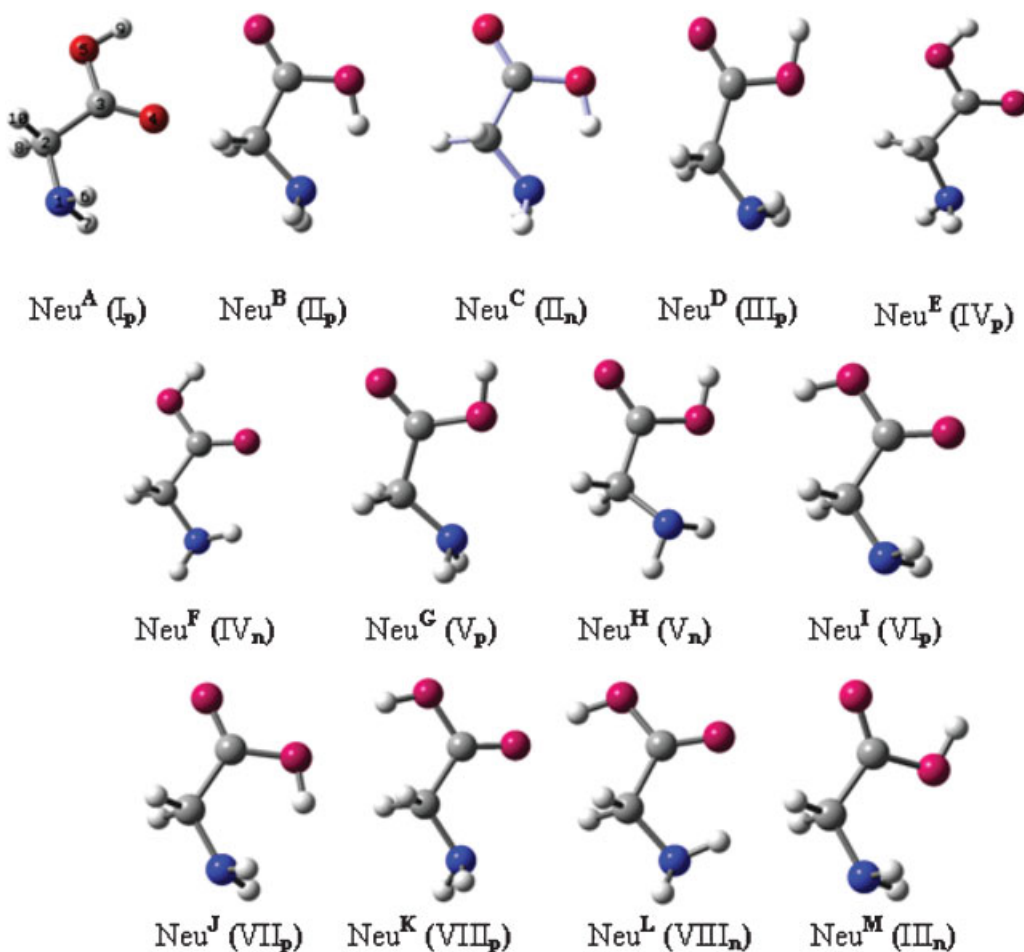


Figure 1. Presentations of glycine neutral structures (Designations of Reference^[10] are listed in parentheses).

The vibrational analyses revealed that some of the geometries are not energy minima at MP2/6-311++G(d,p) theoretical level, and accordingly MP2/cc-pVTZ and CCSD/6-311++G(d,p) methods were used to continue the optimization processes. Subsequently, these geometries were re-optimized under MP2/6-311++G(d,p) theoretical level. The frequency calculations indicated that they are now at energy minima. In this way, the stationary points of all the structures were obtained at the same theoretical level of MP2/6-311++G(d,p), which is a prerequisite for the geometric and energetic comparisons.

RESULTS AND DISCUSSION

The glycine structures at the neutral, deprotonated, α -C radical and carboxylic O radical states were designated to be Neu^A, Dep^A, Rad^A and Rad^A, respectively. As the markers in Figs 1–3 indicate, different conformers of the same state were identified by their superscripts. For example, Neu^A and Neu^B represent two different conformers at the neutral state.

The deprotonation processes to glycine neutral structures

The glycine deprotonated structures were obtained by losing the acidic H₉ atoms from the corresponding neutral structures. At MP2/6-311++G(d,p) theoretical level, the deprotonated structures were degenerated into two independent conformers:

(a) Dep^A, Dep^C, Dep^D, Dep^E, Dep^F, Dep^G, Dep^L and Dep^M, as shown in Fig. 2b; (b) Dep^B, Dep^H, Dep^I, Dep^J and Dep^K, as shown in Fig. 2a. One glycine deprotonated structure at MP2/6-31G(d) theoretical level was previously obtained by Yu *et al.*^[18] The geometries are exactly identical to the structures of Group (a) optimized with the same theoretical methods^[23] whereas show serious discrepancies with the present MP2/6-311++G(d,p) results. It indicates that the diffusion functions are indispensable to treat glycine deprotonated structures and other anionic systems. At MP2/6-311++G(d,p) theoretical level, the total energies and dipole moments of Groups (a) and (b) are exactly equivalent, and the geometric parameters are also identical except when H₆–H₉ atoms are involved. For structures of Groups (a) and (b), H₆ and H₇, H₈ and H₉ are located symmetrically

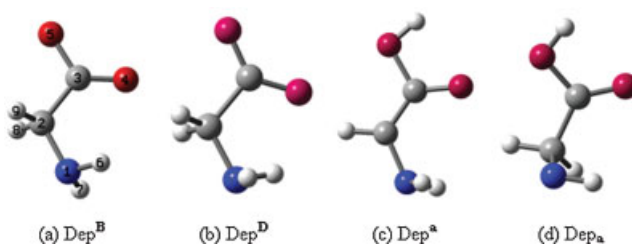


Figure 2. Glycine deprotonated structures.

Table 1. Geometric parameters and spin densities of glycine structures at deprotonated and radical states^a

	Dep ^B	Dep ^D	Rad ^A	Rad ^B	Rad ^E	Rad ^G	Rad ^H	Rad ^I	Rad ^L	Rad ^a	Rad ^d	Rad ^f	Rad ^h
d(N ₁ C ₂)	1.475	1.475	1.360	1.382	1.360	1.363	1.363	1.359	1.359	1.359	1.446	1.455	1.455
d(C ₂ C ₃)	1.561	1.561	1.439	1.467	1.439	1.441	1.441	1.454	1.454	1.454	3.302	1.540	1.523
d(C ₃ O ₄)	1.262	1.262	1.225	1.200	1.225	1.215	1.215	1.213	1.213	1.213	1.169	1.211	1.209
d(C ₃ O ₅)	1.258	1.258	1.360	1.367	1.360	1.372	1.372	1.362	1.362	1.362	1.172	1.327	1.330
d(O ₄ H ₆)	2.265	2.974	2.983	2.209	2.374	2.287	2.287	2.314	2.313	2.313	2.776	2.490	2.490
d(O ₄ H ₇)	2.974	2.265	2.289	115.52	121.06	116.78	121.53	121.53	115.93	115.93	2.774	2.774	107.85
θ(N ₁ C ₂ C ₃)	115.44	115.44	115.44	115.80	124.24	124.34	126.40	122.84	122.83	122.83	125.73	125.55	125.55
θ(C ₂ C ₃ O ₄)	115.41	115.41	115.41	115.80	116.48	115.71	117.27	117.27	115.05	115.05	114.91	110.20	109.50
θ(H ₆ N ₁ C ₂)	103.80	106.71	115.69	115.69	116.48	115.71	117.27	117.27	119.83	119.83	114.75	110.20	110.15
θ(H ₇ N ₁ C ₂)	106.71	103.79	119.46	119.46	115.43	119.46	118.38	118.38	119.83	119.83	114.75	110.20	110.15
ψ(N ₁ C ₂ C ₃ O ₄)	-17.19	17.24	5.01	-116.93	-5.02	-5.59	5.61	5.76	-5.76	-5.76	0.07	-39.27	39.26
ψ(N ₁ C ₂ C ₃ O ₅)	164.84	-164.78	-175.51	11.38	175.49	-175.18	-175.16	-175.12	175.19	175.19	-179.92	142.66	-142.67
ψ(H ₆ N ₁ C ₂ C ₃)	34.48	73.65	-13.88	45.82	13.95	17.49	-17.53	-13.52	13.48	13.48	58.60	52.18	-52.17
ψ(H ₇ N ₁ C ₂ C ₃)	-73.67	-34.49	-162.44	179.88	162.51	164.79	-164.81	-162.12	162.18	162.18	-58.54	170.92	-170.92
Spin(C ₂)				0.834	0.989	0.834	0.827	0.827	0.868	0.868	1.118	0.04	0.03
Spin(O ₄)				0.209	0.288	0.209	0.274	0.274	0.234	0.234	0.002	0.00	-0.00
Spin(O ₅)				0.003	-0.006	0.003	-0.003	-0.004	0.007	0.007	-0.006	1.04	1.05
Dipole moment	3.82	3.82	2.60	6.24	2.60	3.93	3.93	5.39	5.39	5.39	0.99	1.51	3.35

^a Distances in Ångstrom, angles and dihedrals in degree and dipole moments in Debye.

on the N₁C₂C₃O₄O₅ plane (Table 1). Accordingly, structures of Groups (a) and (b) are enantiomers to each other. Compared with the neutral structures, the N₁—C₂ and C₂—C₃ bonds in the deprotonated structures were elongated from *ca.* 1.449 to 1.475 Å and from *ca.* 1.520 to 1.561 Å, respectively. The C₃—O₄ and C₃—O₅ distances in the deprotonated structures become almost equivalent with their exact values of 1.262 and 1.258 Å, respectively, quite different from the situations in the neutral structures, for example, the two distances in conformer Neu^A were optimized at 1.210 and 1.356 Å. In addition, the Mulliken charge analysis indicates that the negative charges were distributed almost evenly on O₄ and O₅ atoms. Therefore, the —COO[—] groups are well conjugated in glycine deprotonated structures.

The glycine neutral and deprotonated structures were connected with each other by deprotonation energies (DE):



$$\text{DE} = E_{\text{dep}} = (\text{Dep}^{\Delta}) - E(\text{Neu}^{\Delta}) \quad (2)$$

where *E*(Neu^Δ) and *E*(Dep^Δ) refer to the total energies of the neutral and their corresponding deprotonated structures, respectively.

At MP2/6-311+G(d,p) theoretical level, the deprotonation energies (*E*_{dep}) of the 13 glycine neutral structures increase in the order Neu^K < Neu^L < Neu^J < Neu^I < Neu^G < Neu^E < Neu^H < Neu^D < Neu^M < Neu^F < Neu^B < Neu^C < Neu^A, with the exact values listed in Table 2. The deprotonation energies vary within the range of 1413.27–1460.03 kJ·mol⁻¹, which agrees well with the experimental value of 1431 kJ·mol⁻¹.^[25,26] Generally, structures with higher deprotonation energies are poorer proton donors and thus show weaker Brønsted acidities. Accordingly, the Brønsted acidities of glycine neutral structures increase as Neu^A < Neu^C < Neu^B < Neu^F < Neu^M < Neu^D < Neu^H < Neu^E < Neu^G < Neu^I < Neu^J < Neu^L < Neu^K. As the two deprotonated structures are of equal total energies, more stable neutral structures will thus have larger deprotonation energies and as a result show weaker Brønsted acidities. Apart from the carboxylic sites, the α-C and amido sites of glycine neutral structures can also be deprotonated, with their deprotonated structures corresponding to Neu^A displayed in Fig. 2c and d. The deprotonation energies of Dep^a and Dep^a were calculated at 1582.02 and 1665.11 kJ·mol⁻¹, respectively, deviating much

Table 2. Absolute and relative (in parentheses) deprotonation energies and RSE^a

	<i>E</i> _{Dep-Δ}	<i>E</i> _{Rad-Δ}	<i>E</i> _{Rad-Δ}
Neu ^A	1460.03 (46.77)	92.24 (47.37)	88.60 (149.82)
Neu ^B	1457.57 (44.30)	45.13 (0.26)	-60.97 (0.26)
Neu ^C	1457.83 (44.56)	44.87 (0.00)	-61.23 (0.00)
Neu ^D	1453.40 (40.13)	90.46 (45.59)	-50.16 (11.07)
Neu ^E	1440.49 (27.23)	111.78 (66.91)	-43.89 (17.34)
Neu ^F	1454.76 (41.50)	97.51 (52.64)	-58.16 (3.07)
Neu ^G	1437.55 (24.29)	106.30 (61.44)	-40.95 (20.28)
Neu ^H	1450.85 (37.59)	93.00 (48.13)	-54.25 (6.98)
Neu ^I	1436.19 (22.92)	88.52 (43.65)	112.44 (173.67)
Neu ^J	1430.92 (17.65)	71.78 (26.91)	-27.68 (33.55)
Neu ^K	1413.27 (0.00)	111.44 (66.57)	-16.66 (44.56)
Neu ^L	1430.41 (17.15)	94.29 (49.42)	-33.82 (27.41)
Neu ^M	1454.00 (40.73)	89.85 (44.98)	-50.76 (10.47)

^a Energy units in kJ·mol⁻¹.

from the experimental value of $1431 \text{ kJ} \cdot \text{mol}^{-1}$.^[25,26] It was also found that the deprotonation energies at the α -C and amido sites are much higher than those at the carboxylic sites, suggesting that the protons of carboxylic O—H groups are more ready to be deprived of compared with those of C—H and N—H groups. It is consistent with the facts that in varieties of molecules including amino acids, the carboxylic O—H groups are the sources to produce Brønsted acidities. Accordingly, the experimental deprotonation energies should be close to the calculated values at the carboxylic sites instead of at the α -C or amido sites. The deprotonated species at the α -C and amido sites will not be considered in the later discussions.

The radicalization processes to glycine neutral structures

α -C radical structures

As shown in Fig. 3a–g, the α -C radical structures were obtained by depriving the H_{10} atoms from the corresponding neutral structures. Altogether seven α -C radical structures were present, and they are (a) Rad^{A} (Fig. 3a); (b) Rad^{B} , Rad^{C} and Rad^{D} (Fig. 3b); (c) Rad^{E} and Rad^{H} (Fig. 3e); (d) Rad^{F} and Rad^{G} (Fig. 3c); (e) Rad^{G} and Rad^{M} (Fig. 3d); (f) Rad^{I} (Fig. 3f); (g) Rad^{K} and Rad^{L} (Fig. 3g). Croft *et al.*^[20] obtained structure Rad^{A} with B3LYP/6-31G(d) methods, of the exactly identical geometries as ours at the same theoretical

level.^[23] It was also found that the α -C radical geometries are not so dependent on the basis sets as the deprotonated geometries.

The N—C distances increase in the order of *ca.* 1.32 \AA in peptides *< ca.* 1.36 \AA in α -C radicals of Groups (a), (c)–(g) *< ca.* 1.38 \AA in α -C radicals of Group (b) *< ca.* 1.45 \AA in glycine neutral structures.^[10] In glycine α -C radicals, the intramolecular delocalized II orbitals were formed between the lone electrons of the N_1 atom and the half-empty 2 p_z orbital of the C_2 atom as well as within the carboxylic groups, as shown in Fig. 4a and b. As to Groups (a) and (c)–(g), the lone orbitals of the N_1 atom and the half-empty orbitals of the C_2 atom were directed in nearly the same direction ensuring the largest overlaps; however, these two orbitals do not match very well in Group (b) and hence the II conjugations were weakened to a certain degree. Analogously, the carboxylic groups in Group (b) are not so well conjugated as in the other groups. In peptides, the intermolecular delocalized II orbitals are formed through the lone electrons of the N atom and the carboxylic group of the anterior amino acid residue, as depicted in Fig. 4c. No obvious conjugations were observed in glycine neutral structures. Accordingly, the sequences of N—C distances above are determined by the degrees of delocalized conjugations.

The total energies of the α -C radicals increase as Group (a) = Group (d) *<* Group (c) = Group (e) *<* Group (f) = Group (g) *<* Group (b). The results of geometric parameters, total energies and dipole

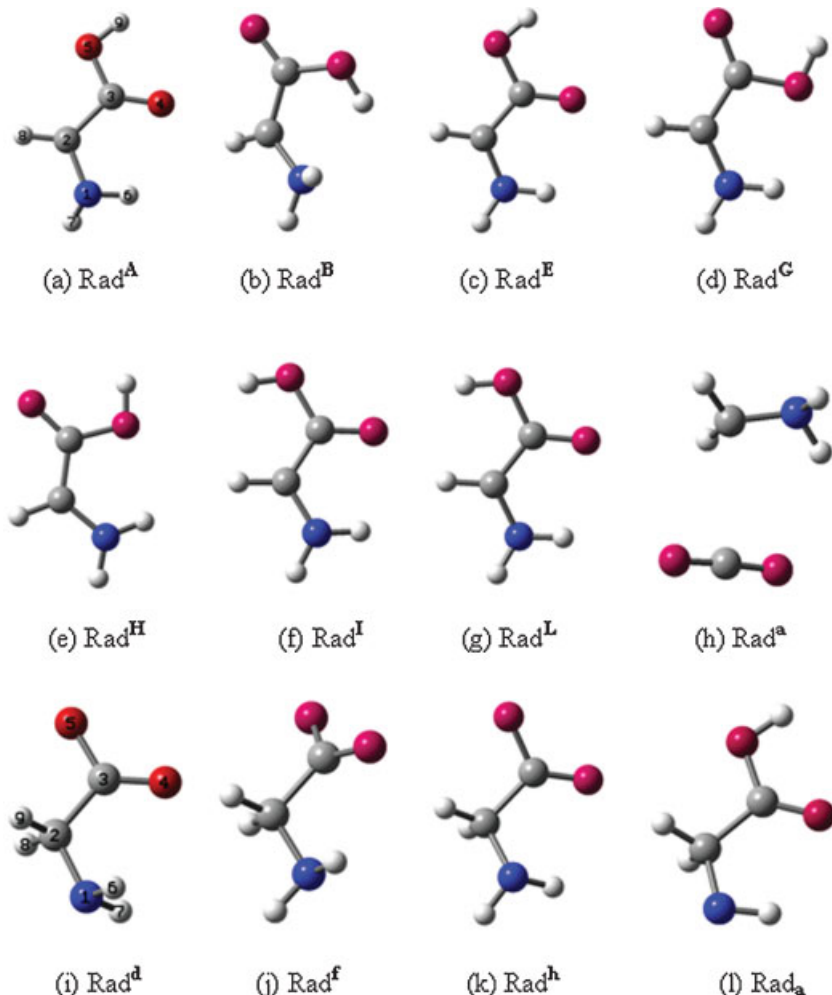


Figure 3. Glycine radical structures.

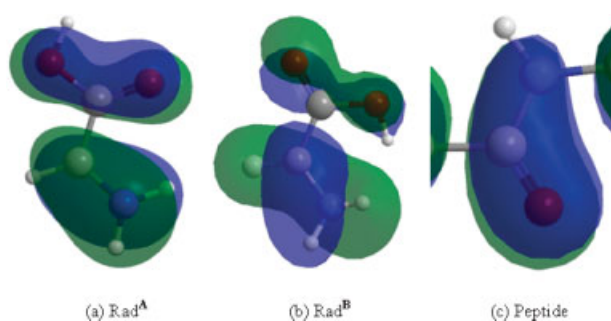


Figure 4. II conjugations in glycine α -C radicals and peptides.

moments imply that structures of Groups (a) and (d), structures of Groups (c) and (e) and structures of Groups (f) and (g) are enantiomers to each other. The highest energies of Group (b) are the natural products of the least conjugation. Groups (f) and (g) are of $27.13 \text{ kJ} \cdot \text{mol}^{-1}$ higher than Groups (a) and (d), probably due to the absence of the O_4-H_9 hydrogen bonds.

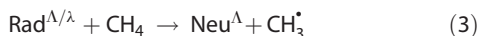
Carboxylic O radical structures

The carboxylic O radicals ($\text{NH}_2\text{CH}_2\text{COO}^\bullet$) differ from α -C radicals in that the radical centers are centered at the carboxylic sites instead of at α -C sites. At MP2/6-311++G(d,p) theoretical level, the glycine carboxylic O radicals were classified into four groups: (a) Rad^a and Rad^i , shown in Fig. 3h; (b) Rad^b and Rad^h , Fig. 3k; (c) Rad^d , Rad^j and Rad^m , shown in Fig. 3i; (d) Rad^c , Rad^e , Rad^f , Rad^g , Rad^k and Rad^l , shown in Fig. 3j. As to Group (a), the structures were cracked into two fragments with the C_2-C_3 bonds ruptured. The θ ($\text{O}_4\text{C}_3\text{O}_5$) angle in Group (a) was calculated to be 178.72° whereas almost linearly (179.73°) in free CO_2 molecule. The two carboxylic C—O distances in Group (a) were optimized at 1.169 and 1.172 Å whereas equivalent in free CO_2 molecule. The geometric deviations of the $\text{O}_4\text{C}_3\text{O}_5$ fragments in Group (a) from free CO_2 molecule are due to the radical centers at the C_3 atoms, which were pre-designed at the O_5 atoms but automatically transferred to the C_3 atoms, see the values of spin densities in Table 1. Accordingly, structures of Group (a) are actually C radicals instead of O radicals. In Groups (b)–(d), the spin densities are mainly localized on the O_5 atoms such that the two carboxylic O atoms are no longer equivalent.

The total energies increase in the order of Group (a) < Group (c) < Group (b) = Group (d). As reported in Reference,^[18] the bond dissociation energies of C—H bonds are much smaller than those of O—H bonds. Structures of Group (a) are C radicals and therefore are of the lowest energies. It was found that there are two hydrogen bonds of H_6-O_4 and H_7-O_4 present in structures of Group (c), which are responsible for the lower energies compared with structures of Groups (b) and (d).

Radical stabilization energies (RSE)

The stabilities of glycine radicals can be estimated and compared with each other through RSE:^[20,27]



$$\text{RSE} = E_{\text{rse}}(\text{Rad}^{\Lambda/\lambda}) = E(\text{Neu}^\Lambda) + E(\text{CH}_3^\bullet) - E(\text{Rad}^{\Lambda/\lambda}) - E(\text{CH}_4) \quad (4)$$

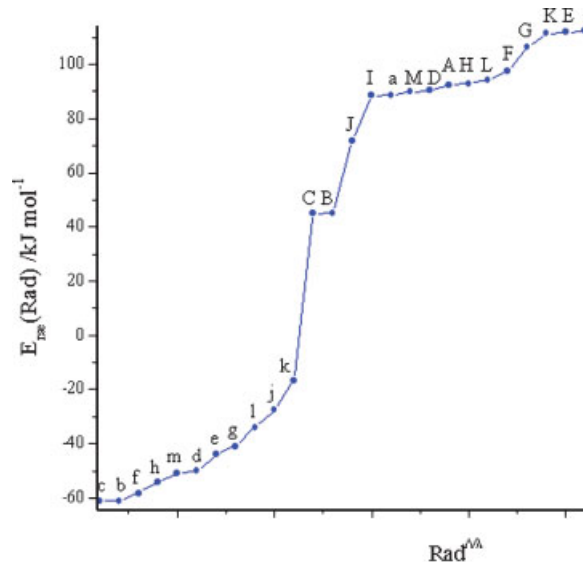


Figure 5. Radical stabilization energies of glycine radicals.

where $E(\text{Neu}^\Lambda)$, $E(\text{Rad}^{\Lambda/\lambda})$, $E(\text{CH}_4)$ and $E(\text{CH}_3^\bullet)$ stand for the energies of glycine neutral structures and the corresponding radicals, CH_4 and its radical, respectively.

The glycine α -C, carboxylic O and C radicals have different RSEs. As shown in Fig. 5, the RSE values increase as $\text{Rad}^c < \text{Rad}^b < \text{Rad}^f < \text{Rad}^h < \text{Rad}^m < \text{Rad}^d < \text{Rad}^e < \text{Rad}^g < \text{Rad}^l < \text{Rad}^j < \text{Rad}^k < \text{Rad}^c < \text{Rad}^b < \text{Rad}^j < \text{Rad}^l < \text{Rad}^a < \text{Rad}^M < \text{Rad}^D < \text{Rad}^A < \text{Rad}^H < \text{Rad}^L < \text{Rad}^F < \text{Rad}^G < \text{Rad}^K < \text{Rad}^E < \text{Rad}^i$, with the absolute and relative RSE values given in Table 2. With MP2/6-31G(d)//B3LYP/6-31G(d) methods, Croft *et al.*^[20] obtained the RSE value of Rad^A at $95.9 \text{ kJ} \cdot \text{mol}^{-1}$, in accord with the present MP2/6-311++G(d,p) data of $92.24 \text{ kJ} \cdot \text{mol}^{-1}$. The RSE values of the carboxylic O radicals are all negative whereas they are positive for the α -C and C radicals, which suggest that the carboxylic O radicals are less stable and therefore are not likely to be produced. The present computational results are consistent with the experimental observations that the C-centred radicals are preferentially formed in biomolecules.^[28,29] The RSE values of α -C radicals vary within the range of 44.87 – $111.78 \text{ kJ} \cdot \text{mol}^{-1}$, with Rad^c being the least stabilized whereas Rad^i the most stabilized. Among all the glycine radicals (Fig. 5), Rad^i is the most stable with its RSE value calculated at $112.44 \text{ kJ} \cdot \text{mol}^{-1}$. Rad^A ranks the seventh most stable, indicating that stable neutral structures are not certain to produce stable radicals. It was found that some neutral structures will not be radicalized at all, for example Neu^c and Neu^b have the lowest RSE values whether at carboxylic O or at α -C sites. In contrast, some neutral structures such as Neu^K are ready to be radicalized at either α -C or carboxylic O site due to the large RSE value at either carboxylic O or α -C site.

The amido sites can also form radicals in the form of $[(\text{NH})\text{CH}_2\text{COOH}]^\bullet$,^[18,21] however, the N radicals are not so ubiquitous as C or O radicals. The amido radical to structure Neu^Λ was displayed in Fig. 3l, which is less stable than Rad^A by $89.17 \text{ kJ} \cdot \text{mol}^{-1}$, agreeing with the BLYP/SVP value of $94.89 \text{ kJ} \cdot \text{mol}^{-1}$.^[21] Such large energy differences indicate that the amido-based radicals are not ready to produce and therefore can be excluded from further discussions, consistent with experimental results.^[28,29] It also agrees with the fact that

Table 3. Populations of glycine structures at neutral, deprotonated and radical states

	$P(\text{Neu}^\Lambda)$	$P(\text{Dep}^\Lambda)$	$P(\text{Rad}^{\Lambda/\lambda})$
1	0.48 (Neu^A)	0.61 ($\text{Dep}^\text{A} + \text{C} + \text{D} + \text{E} + \text{F} + \text{G} + \text{L} + \text{N}$)	0.39 (Rad^A)
2	0.18 (Neu^B)	0.39 ($\text{Dep}^\text{B} + \text{H} + \text{I} + \text{J} + \text{K}$)	0.38 ($\text{Rad}^\text{B} + \text{C} + \text{J}$)
3	0.20 (Neu^C)		0.04 ($\text{Rad}^\text{D} + \text{H}$)
4	0.03 (Neu^D)		0.06 ($\text{Rad}^\text{E} + \text{F}$)
5	1.8E-04 (Neu^E)		0.04 ($\text{Rad}^\text{G} + \text{M}$)
6	0.06 (Neu^F)		2.1E-09 (Rad^I)
7	5.5E-05 (Neu^G)		3.1E-06 ($\text{Rad}^\text{K} + \text{L}$)
8	0.01 (Neu^H)		
9	3.2E-05 (Neu^I)		0.09 ($\text{Rad}^\text{a} + \text{i}$)
10	3.8E-06 (Neu^J)		
11	3.1E-09 (Neu^K)		0.00 ($\text{Rad}^\text{b} + \text{h}$)
12	3.1E-06 (Neu^L)		0.00 ($\text{Rad}^\text{d} + \text{j} + \text{m}$)
13	0.04 (Neu^M)		0.00 ($\text{Rad}^\text{c} + \text{e} + \text{f} + \text{g} + \text{k} + \text{l}$)

the bond dissociation energies of C—H bonds are smaller than those of the O—H and N—H bonds.^[18]

Population analysis

As to glycine neutral structures, the equilibrated populations [$P(\text{Neu}^\Lambda)$] were computed directly with Boltzmann expression:^[9]

$$P(\text{Neu}^\Lambda) = \frac{\exp(-\Delta\varepsilon_{\text{Neu}}/\text{RT})}{\sum_{\Lambda} \exp(-\Delta\varepsilon_{\text{Neu}}/\text{RT})} \quad (5)$$

where $\Delta\varepsilon_{\text{Neu}}$ refers to the energy difference to the most stable conformer, that is $\Delta\varepsilon_{\text{Neu}}(\text{Neu}^\text{A}) = 0$.

It was found that structure Neu^A constitutes nearly half the proportion of all the neutral conformers (Table 3). Instead, the populations of Neu^E , Neu^G , Neu^I , Neu^J , Neu^K and Neu^L can almost be neglected.

The populations of deprotonated structures [$P(\text{Dep}^\Lambda)$] are partially affected by the neutral structures:

$$P(\text{Dep}^\Lambda) = \frac{\sum_{\text{Dep}-\Lambda} P_{\text{Neu}} \cdot \exp(-\Delta\varepsilon_{\text{Dep}}/\text{RT})}{\sum_{\Lambda} \left[\sum_{\text{Dep}-\Lambda} P_{\text{Neu}} \cdot \exp(-\Delta\varepsilon_{\text{Dep}}/\text{RT}) \right]} \quad (6)$$

$$= \frac{\sum_{\text{Dep}-\Lambda} P_{\text{Neu}}}{\sum_{\Lambda} \left(\sum_{\text{Dep}-\Lambda} P_{\text{Neu}} \right)}$$

$\Delta\varepsilon_{\text{Dep}}$ is the energy difference to the most stable deprotonated structure, which equals zero since the two deprotonated structures are of the same energies. The numerator represents the population of one deprotonated structure derived from several neutral structures.

The populations of the two deprotonated structures amount to 61% and 39%, respectively (Table 3). As to Group (a), the deprotonation to structures Neu^A , Neu^C , Neu^D and Neu^M contributes a proportion of 93%, and structures Neu^B and Neu^H in Group (b) constitute nearly 100% proportion.

For each neutral structure, there are two sites of α -C and carboxylic O to be radicalized, and the proportions of α -C and carboxylic O radicals ($P_{\Lambda/\lambda}$) can be calculated with Eqn (7).

Then the population of each radical was obtained with the aid of Eqn (8):

$$P_{\Lambda/\lambda} = \frac{\exp(-\Delta\varepsilon_{\Lambda-\lambda}/\text{RT})}{\sum_{\Lambda+\lambda} \exp(-\Delta\varepsilon_{\Lambda-\lambda}/\text{RT})} \quad (7)$$

$$P(\text{Rad}^{\Lambda/\lambda}) = \frac{P_{\text{Neu}} \cdot P_{\Lambda/\lambda}}{\sum_{\Lambda+\lambda} (P_{\text{Neu}} \cdot P_{\Lambda/\lambda})} \quad (8)$$

$\Delta\varepsilon_{\Lambda-\lambda}$ denotes the energy difference between structures Rad^Λ and Rad^λ .

As shown in Table 3, the populations of all the carboxylic O radicals were calculated to be zero. The populations of all the α -C radicals are positive, although Rad^I , Rad^K and Rad^L are negligible. The α -C radicals of Groups (a) and (b) are comparable in population, indicating the potential roles played by other α -C radicals besides Rad^A ; however, these α -C radicals were neglected in the previous work.^[18,20,21]

CONCLUSIONS

The present *ab initio* calculations concentrated on the deprotonation and radicalization processes on the gaseous glycine structures, with main findings summarized below.

The deprotonation processes to glycine neutral structures will proceed at the carboxylic sites instead of α -C or amido sites. Two carboxylic deprotonated structures of equal energies were obtained with the deprotonation energies calculated within 1413.27–1460.03 kJ·mol⁻¹, which are in good agreement with the experimental results.

The radicalization processes to glycine neutral structures will proceed at α -C sites other than carboxylic or amido sites, consistent with the experimental results. The prevalent oxygen radicals are not ready to form in glycine-related structures. Seven α -C radicals were obtained with RSE calculated within 44.87–111.78 kJ·mol⁻¹.

The population analyses reveal that at neutral or radical state, the major proportions of conformations are due to several most stable structures, suggesting that the other structures can be out of consideration and thus save computational costs.

Acknowledgements

The Talented Funds of Northeast Forestry University (No. 220-602042) and the Chinese Postdoc Foundation (No. 20060400802) are acknowledged.

REFERENCES

- [1] S. Hoyau, G. Ohanessian, *Chem. Eur. J.* **1998**, *4*, 1561.
- [2] M. T. Rodgers, P. B. Armentrout, *Acc. Chem. Res.* **2004**, *37*, 989.
- [3] B. M. Messer, C. D. Cappa, J. D. Smith, K. R. Wilson, M. K. Gilles, R. C. Cohen, R. J. Saykally, *J. Phys. Chem. B* **2005**, *109*, 5375.
- [4] P. D. Godfrey, R. D. Brown, *J. Am. Chem. Soc.* **1995**, *117*, 2019.
- [5] M. Gutowski, P. Skurski, J. Simons, *J. Am. Chem. Soc.* **2000**, *122*, 10159.
- [6] L. Schafer, H. L. Sellers, F. J. Lovas, R. D. Suenram, *J. Am. Chem. Soc.* **1980**, *102*, 6566.
- [7] P. D. Godfrey, S. Firth, L. D. Hatherley, R. D. Brown, A. P. Pierlot, *J. Am. Chem. Soc.* **1993**, *115*, 9687.
- [8] Y. Zubavichus, A. Shaporenko, M. Grunze, M. Zharnikov, *J. Phys. Chem. B* **2006**, *110*, 3420.
- [9] J. Jensen, M. S. Gordon, *J. Am. Chem. Soc.* **1991**, *113*, 7917.
- [10] A. G. Császár, *J. Am. Chem. Soc.* **1992**, *114*, 9568.
- [11] C. H. Hu, M. Shen, H. F. Schaefer, III, *J. Am. Chem. Soc.* **1993**, *115*, 2923.
- [12] V. Barone, C. Adamo, F. Lelj, *J. Chem. Phys.* **1995**, *102*, 364.
- [13] J. J. Neville, Y. Zheng, C. E. Brion, *J. Am. Chem. Soc.* **1996**, *118*, 10553.
- [14] M. Bonifačić, I. Štefanić, G. L. Hug, D. A. Armstrong, K. D. Asmus, *J. Am. Chem. Soc.* **1998**, *120*, 9930.
- [15] F. Jensen, *J. Am. Chem. Soc.* **1992**, *114*, 9533.
- [16] S. Bouchonnet, Y. Hoppilliard, *Org. Mass Spectrom.* **1992**, *27*, 71.
- [17] K. Zhang, D. M. Zimmerman, A. Chung-Phillips, C. J. Cassady, *J. Am. Chem. Soc.* **1993**, *115*, 10812.
- [18] D. Yu, A. Rauk, D. A. Armstrong, *J. Am. Chem. Soc.* **1995**, *117*, 1789.
- [19] K. Zhang, A. Chung-Phillips, *J. Comput. Chem.* **1998**, *19*, 1862.
- [20] A. K. Croft, C. J. Easton, L. Radom, *J. Am. Chem. Soc.* **2003**, *125*, 4119.
- [21] A. Mavrandonakis, S. C. Farantos, G. E. Froudakis, *J. Phys. Chem. B* **2006**, *110*, 6048.
- [22] M. J. Frisch, G. W. Trucks, H. B. Schlegel, G. E. Scuseria, M. A. Robb, J. R. Cheeseman, V. G. Zakrzewski, J. A. Montgomery, Jr., R. E. Stratmann, J. C. Burant, S. Dapprich, J. M. Millam, A. D. Daniels, K. N. Kudin, M. C. Strain, O. Farkas, J. Tomasi, V. Barone, M. Cossi, R. Cammi, B. Mennucci, C. Pomelli, C. Adamo, S. Clifford, J. Ochterski, G. A. Petersson, P. Y. Ayala, Q. Cui, K. Morokuma, D. K. Malick, A. D. Rabuck, K. Raghavachari, J. B. Foresman, J. Cioslowski, J. V. Ortiz, A. G. Baboul, B. B. Stefanov, G. Liu, A. Liashenko, P. Piskorz, I. Komaromi, R. Gomperts, R. L. Martin, D. J. Fox, T. Keith, M. A. Al-Laham, C. Y. Peng, A. Nanayakkara, C. Gonzalez, M. Challacombe, P. M. W. Gill, B. Johnson, W. Chen, M. W. Wong, J. L. Andres, C. Gonzalez, M. Head-Gordon, E. S. Replogle, J. A. Pople, *Gaussian 98, Revision A.9* Gaussian, Inc.: Pittsburgh, PA, **1998**.
- [23] The geometry-optimizations were also performed at lower theoretical levels, i.e., B3LYP/6-31G(d) [20,24] and MP2/6-31G(d) [18], respectively.
- [24] G. Yang, X. W. Han, X. M. Liu, P. Y. Yang, Y. G. Zhou, X. H. Bao, *J. Phys. Chem. B* **2005**, *109*, 18690.
- [25] M. J. Locke, R. T. McIver, Jr., *J. Am. Chem. Soc.* **1983**, *105*, 4226.
- [26] S. Campbell, R. Renneboog, P. Kebarle, *Can. J. Chem.* **1989**, *67*, 611.
- [27] C. J. Parkinson, P. M. Mayer, L. Radom, *J. Chem. Soc. Perkin Trans. 2* **1999**, 2305.
- [28] M. Schwarzberg, J. Sperling, D. Elad, *J. Am. Chem. Soc.* **1973**, *95*, 6418.
- [29] C. J. Easton, M. P. Hay, *Chem. Commun.* **1986**, 55.